In situ and *real-time* visualisation of oxygen distribution in DMFC using a porphyrin dye compound†

Junji Inukai,[a] Kenji Miyatake,[a] Yuta Ishigami,[a] Masahiro Watanabe,*[a] Tsuyoshi Hyakutake,[b] Hiroyuki Nishide,[b] Yuzo Nagumo,[c] Masayuki Watanabe[c] and Akira Tanaka[d]

Received (in Cambridge, UK) 3rd December 2007, Accepted 18th January 2008
First published as an Advance Article on the web 11th February 2008
DOI: 10.1039/b718692d

A luminescent porphyrin dye film has been coated onto a transparent separator on the cathode side of a direct methanol fuel cell (DMFC) to visualise clearly oxygen distribution under operating conditions by analysing emission from the dye.

Direct methanol fuel cells (DMFCs) generate electric power *via* chemical reaction of methanol (MeOH) and oxygen and thus, are considered to be a promising power source for portable devices.[1,2] However, there are at least two major issues to be solved before the commercialisation of DMFCs; *i.e.*, insufficient electrocatalytic activity (for both oxygen reduction and MeOH oxidation reactions)[3–5] and substantial MeOH cross-over (permeation) through the polymer electrolyte membrane, resulting in a direct combustion of MeOH.[6] The MeOH cross-over lowers not only fuel efficiency but also voltage efficiency due to the mixed potential of oxygen reduction and MeOH oxidation reactions at the cathode. In order to analyse the current problems and achieve higher performance DMFCs, it is desired to monitor the MeOH cross-over and oxygen partial pressure in the cathode reaction field.

In this communication, we report a novel analytical system which visualises *in situ* oxygen distribution in an operating DMFC through a non-destructive method.[7] The change in oxygen partial pressure reflects oxygen consumption *via* electrochemical reaction and *via* direct combustion of crossed-over MeOH, as well as oxygen supply conditions. As an oxygen probe, we used a luminescent dye compound, [tetrakis(pentafluorophenyl)porphyrinato]platinum (Fig. 1(a)) which absorbs blue light (λ_{max} = 380 nm in Soret band) and emits red light (ε_{max} = 650 nm).[8] The emission intensity corresponds to the oxygen partial pressure of the atmosphere. The dye was dispersed into poly(1-trimethylsilyl-1-propyne)[9–13] (Fig. 1(b)) which was chosen as a matrix because of its high oxygen permeability, compatibility with the dye, good film forming capability, and stability under DMFC conditions.

The composition of DMFC used for the experiment is depicted in Fig. 2. A 3 × 3 cm^2 membrane electrode assembly (MEA) was sandwiched by two transparent separators. In this experiment, we used two different kinds of membranes, aromatic hydrocarbon polymer with sulfoalkylene groups[14] and fluorocarbon ionomer (Nafion 117). A dye film was coated on a transparent separator (on the cathode side) with open slits as a passive air supply. Therefore, the oxygen partial pressure beneath the separator was visualised.

The cell surface was placed in a transparent polyacrylate-resin enclosure to supply oxygen gas with controlled partial pressure. A schematic illustration of the phosphorescence imaging system for measuring the oxygen partial pressure is provided in the ESI† (Fig. S1). A laser beam (407 nm) was diffused, spread and distributed uniformly (50 μW cm^{-2}) onto the separator. The emission from the dye film through the transparent separator was filtered (> 600 nm) and images were captured with a charge-coupled device (CCD) camera (1 pixel = approximately 0.1 mm).

The cell was initially supplied with a mixture of air and nitrogen at various ratios to obtain a calibration curve, known as a phosphorescence quenching or Stern–Volmer plot,[15] for every pixel under the ribs. During the calibration curve measurements, the anode was supplied with pure water. In order to eliminate the effect of water permeating from the

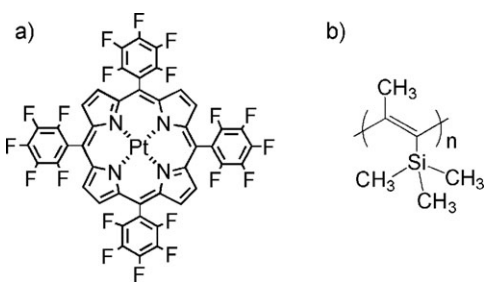

Fig. 1 Chemical structures of [tetrakis(pentafluorophenyl)porphyrinato]platinum (a) and poly(1-trimethylsilyl-1-propyne) (b).

[a] *Clean Energy Research Centre, University of Yamanashi, 4 Takeda, Kofu, Yamanashi 400-8510, Japan. E-mail: m-watanabe@yamanashi.ac.jp; Fax: 81-55-254-0371; Tel: 81-55-220-8620*
[b] *Department of Applied Chemistry, Waseda University, 3-4-1 Okubo, Shinjuku, Tokyo 169-8555, Japan. E-mail: nishide@waseda.jp; Fax: 81-3-3209-5522; Tel: 81-3-3200-2669*
[c] *Technology Research Laboratory, Shimadzu Corporation, 3-9-4 Hikaridai, Seika-cho, Kyoto 619-0237, Japan. E-mail: ynagumo@shimadzu.co.jp; Fax: 81-774-95-1669; Tel: 81-774-95-1668*
[d] *Hitachi Laboratory, Hitachi Limited, 1-1-1 Omika-cho, Hitachi, Ibaraki 319-1292, Japan. E-mail: akira.tanaka.xv@hitachi.com; Fax: 81-294-52-7624; Tel: 81-294-52-5111 (ext: 5751)*

† Electronic supplementary information (ESI) available: Experimental details, optical system, calibration curves (Stern–Volmer plots), and transient response of oxygen distribution (movie). See DOI: 10.1039/b718692d

 This journal is © The Royal Society of Chemistry 2008

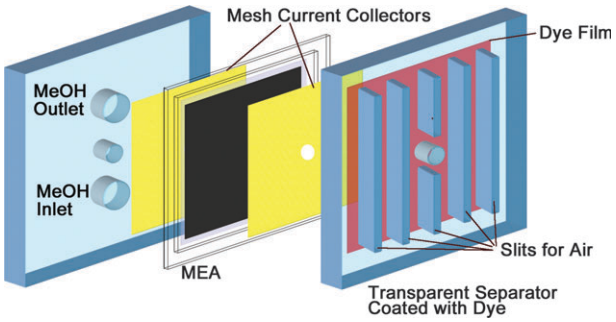

Fig. 2 Composition of a DMFC for visualisation of oxygen distribution.

anode through the membrane, the mixed gas supplied to the cathode was fully humidified. The partial pressure of water vapour, as well as that of nitrogen, was subtracted from the atmospheric pressure for the calculation of the oxygen partial pressures in the system. In this way, the relationship between the emission intensity from the dye film and the actual oxygen partial pressure was obtained at every pixel, or every 0.1 × 0.1-mm^2 point. Each curve was then fitted with a cubic polynomial (ESI,† Fig. S2).

After obtaining calibration curves, the gas was changed to dry air, and 10 wt% MeOH was supplied into the anode instead of water. Fig. 3 shows the distribution of emission intensity for the DMFC. Hydrocarbon and fluorocarbon membranes were used for Fig. 3(a)–(c) and (d)–(f), respectively. The white square indicates the position of the MEAs. The feature in the lower middle of the image is a wire connected to the centre of the current collector mesh. The emission intensity became higher when the anode flow was changed from water to 10 wt% MeOH (Fig. 3(b) and (e)), indicating that the oxygen was consumed by the oxidation of MeOH crossing over from the anode through the membrane. When the cell was operated, the current density obtained ranged up to 90 mA cm^{-2} for the hydrocarbon membrane and up to 50 mA cm^{-2} for the fluorocarbon membrane. The difference in the attainable current densities was due to the

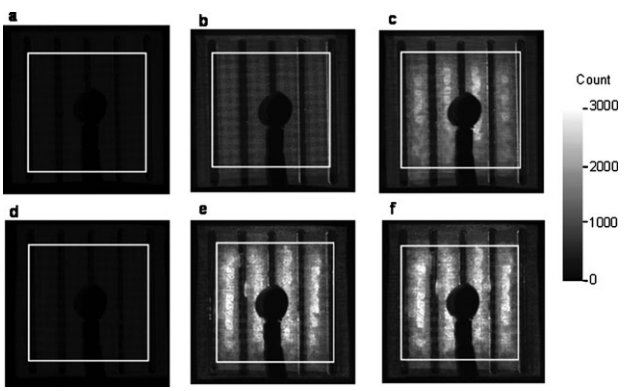

Fig. 3 Emission intensity from the dye film on a DMFC: cell temperature = room temperature; fuel = 10 wt% MeOH; with a hydrocarbon membrane (a: no MeOH, b: current density = 0 mA cm^{-2}, c: current density = 90 mA cm^{-2}); with a fluorocarbon membrane (d: no MeOH, e: current density = 0 mA cm^{-2}, f: current density = 50 mA cm^{-2}).

different amounts of MeOH crossing over through the membranes (see below). The intensity became even higher when the cell was operated (Fig. 3(c) and (f)), due to the electrochemical reaction of oxygen with protons and electrons producing water.

After data acquisition, the emission intensity from the dye film under the ribs was transformed to the oxygen partial pressure using the calibration curves described above. Fig. 4 shows the oxygen partial pressure distribution for the DMFC beneath the separator. When water was introduced in the anode, the oxygen partial pressure was already seen to decrease using the fluorocarbon membrane, as in Fig. 4(d), because of the penetration of water from the anode to the cathode. In contrast, water penetration was very low for the hydrocarbon membrane (Fig. 4(a)), because the partial pressure of oxygen in the cathode was comparable to that of dry air in the entire area. At open circuit (Fig. 4(b) and (e)), oxygen consumption was observed more clearly and quantitatively. It should be noted that the oxygen consumption by crossed-over MeOH was more pronounced with the fluorocarbon membrane (Fig. 4(e)) than with the hydrocarbon membrane (Fig. 4(b)): oxygen partial pressure was about 10 kPa for the hydrocarbon membrane, while that for the fluorocarbon membrane was lower than 2 kPa. The regions in black (some regions are circled in Fig. 4(e)) shows the formation of liquid water, which was verified by an optical examination. Thus, the degree of undesirable MeOH cross-over was clearly visualised with this new technique. These observations are not contradictory to the common understanding that non-fluorinated or hydrocarbon membranes are less permeable to MeOH and water than fluorocarbon membranes.[6,16]

The patterns of oxygen partial pressure in the running DMFCs were also obtained, as shown in Fig. 4(c) and (f): the oxygen partial pressure was the lowest in the middle of the MEA. As noted above, for the hydrocarbon membrane, the current density was as high as 90 mA cm^{-2}, *vs.* 50 mA cm^{-2} for the fluorocarbon membrane, due to the lack of oxygen in the centre of the MEA, as a result of consumption by crossed-over MeOH. At current densities larger than these values, the oxygen partial pressure approached zero in the middle of the MEA in both cases. Because of the pronounced penetration of MeOH, the largest current density obtained using the fluorocarbon membrane was only half that using the hydrocarbon membrane. Liquid water was also formed. Under these conditions, the cell performance became unstable and operation could not be continued.

Fig. 5 shows the oxygen partial pressures at four selected points under the ribs when the current density was stepped to 40 and 80 mA cm^{-2} for the simulation of startup–shutdown cycles (hydrocarbon membrane). Images were obtained every 0.5 s (Movie S1 in the ESI†). On open circuit, the oxygen partial pressure was lower at points 1 and 3, indicating uneven flow of aqueous MeOH (efficient flow at points 1 and 3). When the current density was increased to 40 mA cm^{-2}, the oxygen partial pressure decreased more slowly at point 2 since it was located nearer to the slit and had a better oxygen supply. Because oxygen consumption is a function of current density and MeOH cross-over, the oxygen partial pressures reversed for points 2 and 3 compared to those at OCV. A significant

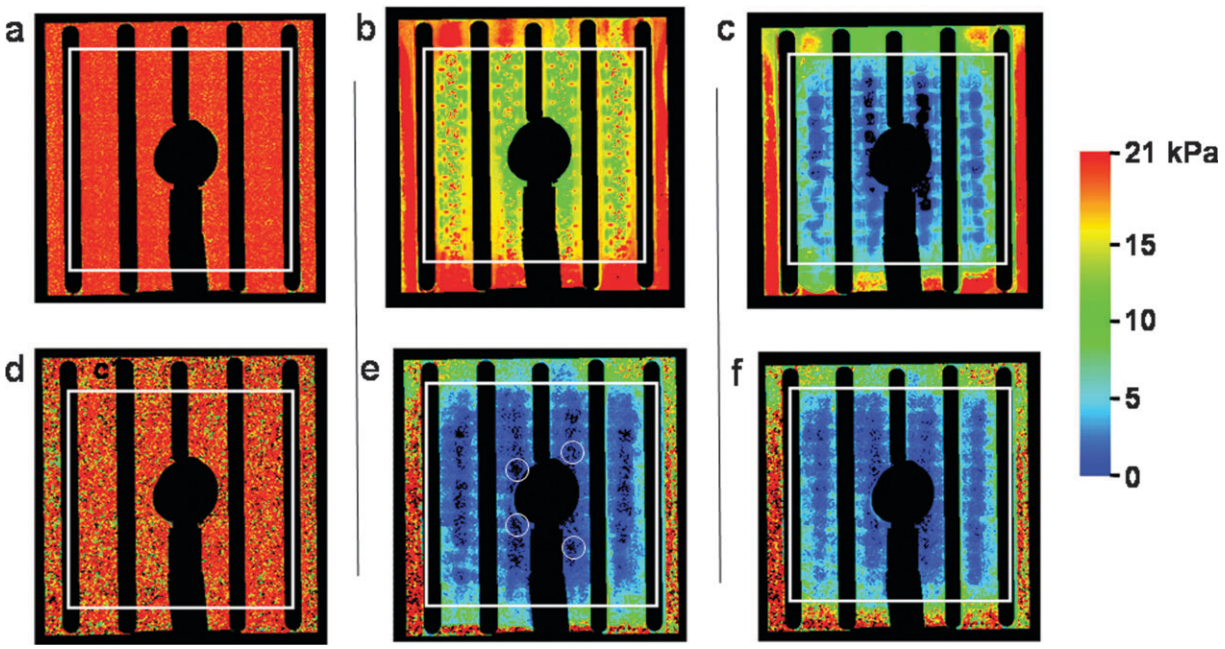

Fig. 4 Oxygen partial pressures visualised in an operating DMFC (conditions are the same as in Fig. 3).

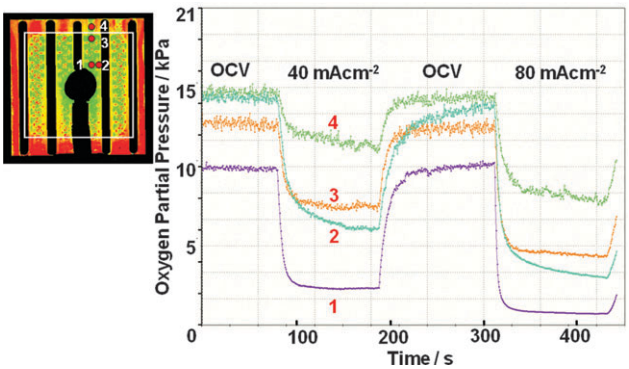

Fig. 5 Oxygen partial pressures at four points (points 1–4) beneath the transparent separator during the simulation of startup-shutdown cycles for a DMFC (hydrocarbon membrane); current densities were stepped to 40 and 80 mA cm^{-2}; measured area = 1.0 × 1.0 mm.

amount of oxygen was also consumed at point 4 (outside the MEA or reaction field), indicating oxygen flow from outside to inside the MEA through the gas diffusion medium (carbon paper). An attempt to quantitatively describe the MeOH cross-over is now in progress using MeOH solutions of different concentrations.

In summary, we have successfully visualised oxygen distribution in an operating DMFC. Higher oxygen consumption due to MeOH cross-over was clearly confirmed for the fluorinated membrane than for the hydrocarbon membrane, which limits the attainable current density, and accordingly, cell performance. The transient experiments revealed an uneven flow of MeOH solution and thus the necessity of a better cell structure. This technique is directly applicable to proton electrolyte fuel cells and such attempts will be reported elsewhere.[17] The simultaneous visualisation of these parameters is expected to become a very effective tool to achieve accurate analyses of DMFC operation, and eventually higher performance.

This study was supported by the New Energy and Industrial Technology Development Organization (NEDO), Japan. The authors thank Mr K. Takada for his experimental help and Profs D. A. Tryk, A. Wieckowski, P. P. Edwards, D. J. Schiffrin and T. Zawodzinski for their comments.

Notes and references

1 A. S. Arico, S. Srinivasan and V. Antonucci, *Fuel Cells*, 2001, **1**, 133.
2 S. Gottesfeld, *Encycl. Electrochem.*, 2007, **5**, 544.
3 K. R. Williams and G. T. Burstein, *Catal. Today*, 1997, **38**, 401.
4 R. Dillon, S. Srinivasan, A. S. Arico and V. Antonucci, *J. Power Sources*, 2004, **127**, 112.
5 H. Liu, C. Song, L. Zhang, J. Zhang, H. Wang and D. P. Wilkinson, *J. Power Sources*, 2006, **155**, 95.
6 N. W. Deluca and Y. A. Elabd, *J. Polym. Sci. B: Polym. Phys.*, 2006, **44**, 2201.
7 *Pressure and Temperature Sensitive Paints*, ed. T. Liu and J. P. Sullivan, Springer, Berlin, 2005.
8 K. Asai, Y. Amao, Y. Iijima, I. Okura and H. Nishide, *J. Thermophys. Heat Transfer*, 2002, **16**, 109.
9 T. Masuda, E. Isobe and T. Higashimura, *J. Am. Chem. Soc.*, 1983, **105**, 7473.
10 Y. Amano, K. Asai, I. Okura, H. Shinohara and H. Nishide, *Analyst*, 2000, **125**, 1911.
11 K. Nagai, T. Masuda, T. Nakagawa, B. D. Freeman and I. Pinnau, *Prog. Polym. Sci.*, 2001, **26**, 721.
12 Y. Amano, I. Okura, H. Shinohara and H. Nishide, *Polym. J.*, 2002, **34**, 411.
13 T. Niimi, M. Yoshida, M. Kondo, Y. Oshima and H. Mori, *J. Thermophys. Heat Transfer*, 2005, **19**, 9.
14 T. Koyama, M. Morishima, S. Suzuki and H. Honbou, *IEICE Tech. Rep. Component Parts Mater.*, 2006, **105**, 7.
15 *Topics in Fluorescence Spectroscopy Volume 2: Principles*, ed. J. R. Lakowicz, Springer, Berlin, 1991.
16 K. Miyatake, H. Zhou, T. Matsuo, H. Uchida and M. Watanabe, *Macromolecules*, 2004, **37**, 4961.
17 J. Inukai, K. Miyatake, K. Takada, M. Watanabe, T. Hyakutake, H. Nishide, Y. Nagumo, M. Watanabe, M. Aoki and H. Takano, *Angew. Chem., Int. Ed.*, 2008, in press.

 This journal is © The Royal Society of Chemistry 2008